A ^{1}H NMR relaxometry investigation of gel-pore drying shrinkage in cement pastes.

A. M. Gajewicz[*], E. Gartner[#], K. Kang[*], P. J. McDonald[*$], V. Yermakou[#§]

[*] Department of Physics, University of Surrey, Guildford, Surrey, GU2 7XH, UK

[#] LafargeHolcim Research Centre, 95 rue du Montmurier, 38291 St Quentin Fallavier Cedex, France

[§] Micro and NanoMaterials and Technologies Industrial Doctorate Centre, University of Surrey, Guildford, Surrey, GU2 7XH, UK

[$] Corresponding author

Abstract

The first systematic study of the temporal evolution of the pore-size-distribution (PSD) in mature cement pastes following one and two cycles of drying and rewetting is presented. The PSD is measured using ^{1}H nuclear magnetic resonance (NMR) relaxometry. For millimetre sized paste samples dried fairly strongly, the volume of water taken up shortly after rewetting slightly exceeds the pre-drying amount. The volume of water in pores > 10 nm far exceeds that in smaller pores. This reverses the situation observed prior to drying. Over subsequent days the water distribution reverts to its original form, so that the dominant fraction is again in the smaller pores. Since the total water content scarcely changes, this indicates a re-arrangement of the nano-scale porosity. Over two drying-rewetting cycles, both reversible and irreversible changes are seen. The effect is not observed in moderately dried pastes.

Introduction

A better understanding of the shrinkage of cementitious materials when exposed to the ambient environment is of practical engineering importance for their use in construction. Shrinkage can lead to cracking [1] that in turn can accelerate degradation processes which may ultimately impair structural integrity if no remedial measures are taken. Shrinkage at constant temperature can be divided into two major categories: autogeneous shrinkage, which occurs during hydration of sealed samples and is thus essentially a homogeneous process caused by hydration and not related to loss of water by evaporation; and drying shrinkage, which results from the evaporation of water into the external environment and is thus inhomogeneous and highly sensitive to relative humidity gradients. However, both forms of shrinkage involve the same basic components that come into play at different states of water saturation and which can be correlated with different parts of the water sorption isotherm as a function of relative humidity, and thus with specific equivalent pore size ranges [2-4]. Both drying shrinkage and water sorption exhibit reversible and irreversible components as well as reversible hysteresis as a function of relative humidity at constant temperature. However the irreversible component is mainly limited to the first drying step [5]. These phenomena are believed to be mainly due to the volume changes in the calcium-silicate-hydrate (C-S-H) gel which constitutes the principal matrix phase in cement paste (which is itself the principal matrix phase in concretes and mortars) and which has a complex porous microstructure capable of significant evolution with time and with changing conditions of humidity and temperature. However the lack of clear methods to investigate quantitatively such a complex microstructure has inhibited substantive progress in understanding these phenomena.

Nuclear magnetic resonance (NMR) ^{1}H relaxometry has been shown to be a powerful tool for the quantitative characterisation of the nano- and micro-porosity of cement pastes [6] thanks to proportionality between the ^{1}H relaxation rate of water in pore spaces and the pore surface to volume ratio. This proportionality, that is based on an averaging of the relaxation rate of a few rapidly relaxing molecules adsorbed on the pore surface and many more slowly relaxing molecules in the pore bulk is well established for many materials types. It is explained in the pioneering works of Zimmerman and Brittin, [7], Brownstein and Tarr [8] and D'Orazio *et al*. [9].

In one particular study of cement, the NMR sorption isotherm was measured [10,11]. The total signal strength was shown to correlate with the total adsorbed water as a function of humidity throughout the first drying and wetting cycle. Moreover, the signal was decomposed into fractions of water in different pore type environments so that a pore-size resolved isotherm could be measured. The key advantage of the method is that the probe is the water inherent in the sample. The method is non-destructive so enabling time course studies in as-prepared materials without recourse to drying if so wished. Basic experiments are quick (minutes) and may be carried out on relatively inexpensive bench-top equipment. Recent reviews describe the technique in ways targeted at the cement-user community [12,13].

In this report we describe the first systematic study of the time-dependent changes in C-S-H porosity occurring in cement paste *after* a cycle of drying and rewetting. The study is carried out using laboratory bench-top low-field ^{1}H NMR relaxometry. The work was inspired by the recent results of Fischer *et al.* [14] who reported unilateral surface GARField and laboratory GARField ^{1}H NMR measurements of concrete and mortar samples that showed an

immediate (1-day) increase in capillary water upon rewetting samples after initial drying and compared to pre-drying. This increase then fell back towards pre-drying levels over the subsequent 2 to 7 days. The use of a GARField system enabled the measurements to be made with spatial resolution. Spatial resolution allowed discernment of local changes in porosity as a wetting front passed during water ingress experiments. The changes would not have been seen without spatial localisation. The bulk ingress of water would have masked the effect. However, the use of GARField inhibited accurate assessment of the state of water in the very smallest pores, so that only one side of the story was revealed. Bench top ^{1}H NMR allows all the porosity to be measured, including the smallest gel pores but at the expense of requiring small samples that are implicitly assumed to be uniformly saturated.

Samples are measured immediately before drying and during re-wetting. The results indicate that there is reorganisation of the microstructure of cement hydrate gel after rewetting compared to before drying. The changes are biggest in samples that are dried to a state of empty gel pores and interlayer spaces. The results also show that a substantial fraction, but not all, of the changes are reversible on a timescale of 24 - 48 hours after rewetting. Measurements have been made, and changes seen over two cycles of drying and wetting.

The story that emerges complements, and takes further, recent work of Maruyama *et al*. [15] and Jennings *et al.* [16]. Maruyama *et al.* published a comprehensive study of microstructural and bulk property (especially length) changes in hardened cement paste measured using a range of techniques during the first drying. They conclude that during first drying there is an increase in the volume of larger pores and a decrease in the volume of smaller pores. Working with the colloidal model of cements [4], they attribute the former to

93 a consolidation of C-S-H globules and the latter to a densification of C-S-H within individual
94 globules but note too that the results are consistent with the alternate microstructural
95 model due to Feldman and Sereda [17]. By studying the different effects of short (hours)
96 and long (months) term drying they separate the effects of shrinkage from microstructural
97 rearrangements. Jennings *et al.* also showed how a careful analysis of sorption isotherm
98 cycles could be used to infer microstructural changes and information on drying shrinkage.
99 They additionally make the observation that water in interlayer spaces does not dry from
100 the C-S-H above a relative humidity (RH) of circa 25%, a result that confirms previous
101 conclusions drawn from NMR data [10], and go on to say that, once removed, this water
102 does not fully resaturate these spaces, even at 100% RH. This later conclusion is less clearly
103 supported by the NMR evidence. Our new work reported here augments these earlier
104 studies by looking at the time dependence of microstructural changes that occur during
105 water adsorption, following desorption.

106 **Methods**

107 Two completely independent sets of samples were prepared and analysed for the first
108 sorption cycle: one in the Surrey University laboratories (NMR frequency 20 MHz) and one
109 in the LafargeHolcim laboratories (NMR frequency 23.5 MHz). The results are in excellent
110 agreement. Thereafter, the severity of drying was investigated at LafargeHolcim, the second
111 sorption cycle at Surrey.

112 The materials and methods are given for samples prepared in the Surrey laboratories. Minor
113 differences for samples made at LafargeHolcim are presented as footnotes. White cement
114 powder with the composition: 62.9% C_3S; 19.1% C_2S; 7.2% C_3A; 5.2% C$·0.5H; 2.4% CH and

115 2.2% $C\bar{C}$ was used[1]. Typically water was added to 80 g of the anhydrous cement in the water
116 to cement (*w*/*c*) ratio 0.4 by mass and mixed using the protocols established by Nanocem
117 (www.nanocem.org) and published by us elsewhere [10]. Samples were cast in moulds of
118 about 1 cm^3 volume and curing begun at room temperature under a small excess of
119 saturated calcium hydroxide (CH) solution[2] which was added about 1 hour after casting, just
120 as the sample was starting to set, in order to compensate for water taken up by the
121 hydration reaction. After 1 day, the samples were transferred with solution to small, sealed
122 containers for convenience and curing continued for a total of 28 days at 20 ± 1°C. At the
123 end of the curing period, samples were individually crushed into millimetre-sized pieces to
124 enable subsequent rapid drying and re-wetting and to avoid the problems associated with a
125 spatially non-uniform distribution of water that occurs for larger samples, which might mask
126 the effects we seek to measure. For instance, during wetting of a large sample, the
127 evolution of porosity change near a water ingress front would be at a much "younger" stage
128 of development than near the sample surface as the surface would have contacted water
129 for a longer period. Crushed samples were measured by NMR "as-prepared".

130 Crushed samples were subsequently dried. Drying methods were used as follows: drying at
131 60°C under slightly reduced pressure (0.85-0.95 bar) for an extended period of one month;
132 drying at either 40°C or 60°C under slightly reduced pressure for a short period of 2 or 3
133 days respectively; drying at room temperature in a 23% relative humidity (RH) environment
134 for 3 days; and slow drying over saturated salt solutions and silica gel[3] by progressive
135 lowering the RH down to about 15% over a period of about 1 month. Previous NMR work

[1] 65.3% C_3S; 26.9% C_2S; 2.9% C_3A; 2.1% CH and 0.8% $C\bar{C}$; 1.4% $C\bar{S}$ at LafargeHolcim
[2] PURELAB® water was used at LafargeHolcim
[3] KH_2PO_4 (~96% RH); $(NH_4)_2SO_4$ (~80%); $Mg(NO_3)_2$ (~55%) ; $MgCl_26H_2O$ (~33%)[18,19]. Silica gels 23 and 15% measured.

suggests that drying for a short period at 40°C to 60°C or at 23% RH is sufficient to remove water from the gel porosity but not to remove water from the C-S-H inter-layer spaces [10,20].

Dried samples were measured by NMR and then immersed in, and stored under, saturated CH solution[2] in order to rewet them. They were only removed from the solution for the brief periods (a few minutes) necessary for NMR measurements at various wetting times.

For ^{1}H NMR relaxometry measurements, the crushed pieces of sample (the same pieces for any one experimental series) were dabbed dry with filter paper and placed in the bottom of a 10 mm diameter NMR tube. The free space was taken up by a solid glass rod to limit evaporation into the space above the sample and the whole assembly sealed with Parafilm®. A Carr-Purcell-Meiboom-Gill (CPMG) pulse sequence experiment was used for all measurements. As we have previously shown, the ^{1}H T_2 relaxation time distribution can be calculated from the measured CPMG echo sequence decay and directly reflects the pore size distribution of water filled porosity in the sample. The typical π/2 pulse length, $t_{\pi/2}$, was 5 μs; 256 log-spaced echoes were recorded from 60 μs to 880 ms; the experimental repetition time was 1 s and 512 averages were recorded. With these parameters it took about 8.5 minutes to record the CPMG data[4]. Additionally, when the measurement was not thought to be time-critical, in so much as the water distribution was not expected to change significantly during the measurement period, a quadrature echo sequence was also run. From this experiment it is possible to determine additionally the fraction of all hydrogen protons combined in crystalline hydrates such as Portlandite (calcium hydroxide) and ettringite. Here, single quadrature or "solid" echoes were recorded for pulse gaps, τ, in the

[4] π/2: 6.5 μs; echo range 58 μs to 65 ms; 1024 averages at 0.565 s repetition time taking 9.6 minutes at LafargeHolcim

158 range 12 to 54 μs. The signals were decomposed into “solid” and “liquid” fractions, and
159 these were extrapolated back to zero pulse gap using Gaussian and exponential curves
160 respectively. Further details of the measurement and analysis procedures are to be found in
161 the literature [12,13]. Samples were weighed at every significant point of the sample
162 preparation and measurement process.

163 The CPMG data can be analysed in multiple ways. That which makes the least *a priori*
164 assumptions about the results involves an inverse Laplace transform of the echo decay to
165 reveal the quasi-continuous T_2 distribution. We have previously analysed much data this
166 way. The major problem is that the method requires a signal-to-noise ratio (SNR) in excess
167 of several hundred. Here we have used small pieces of crushed sample which immediately
168 lowers the SNR per scan. We have not wanted to increase the number of averages unduly
169 for fear of changing the water or porosity distribution during the measurement time. Also,
170 some samples were very dry, limiting the SNR for want of signal from water in the sample.
171 With lower SNR, peaks in the inverse Laplace transform can become broadened or merged
172 masking the effects we seek to measure. In consequence, in addition to inverse Laplace
173 analysis, we have also performed constrained multi-exponential fitting using as constraints
174 the expected number of peaks and the T_2 relaxation time values of as prepared material
175 now well-known from earlier published studies [6,21].

176 The exponential fitting was constrained as follows. First, the “as-prepared” material was fit
177 to a four component exponential decay for which the three shortest time constants were
178 forced in the ratio 1:3:9. The actual relaxation time values of water in the smallest pores
179 depend on the pore size and level of paramagnetic impurities in the sample. However,
180 previous work says that they occur in this ratio, associated with, in order, water in interlayer

~~spacing~~ spaces in the gel hydrates, water in gel pores and water in interhydrate pores[5]. The fourth time constant was set equal to 40 ms – a generic value for large pores that has marginal effect on the quality of the data fitting. The amplitudes were left to float, so making a fit with 5 free parameters (4 amplitudes and the shortest time constant). Thereafter, the time constants were maintained fixed across a sample set so that in analysis of re-wet material only the 4 amplitudes were varied.

Results

(a) C-S-H desorption-adsorption cycle and swelling.

[5] This assignment pre-supposes that the water reservoirs associated with different pore sizes are isolated. In practice, pores of different size are connected and there is exchange of water / nuclear magnetisation between them. The critical observation is that this exchange is slow as was previously demonstrated, and indeed exploited, to measure the inter pore exchange rate [22]. Distinct relaxation modes are seen. If the exchange were fast compared to the relaxation rate, then a single relaxation mode with an average relaxation time reflecting the combined pore size would be observed. In the case of the C-S-H interlayer space, the discussion in the paper is in terms of ^{1}H in water. However, this does not preclude ^{1}H in silanol groups. While the small size of the interlayer may cause a small systematic error in the calculation of the pore size due to the absence of an identifiably "bulk" water reservoir in the pore and uncertainty about the surface relaxivity, it does not alter the fact that a distinct relaxation reservoir is observed.

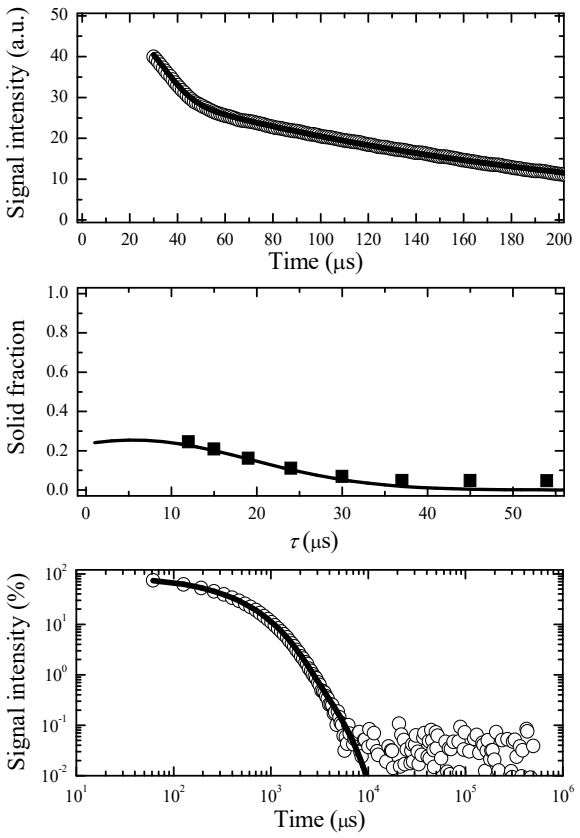

Figure 1: A quadrature echo decay for an "as-prepared" sample for τ = 12 μs (top); the solid fraction as a function of τ together with back extrapolation to $t_{\pi/2}$ pulse gap (middle); and a log-log plot of the CPMG decay together with a constrained multi-exponential fit as described in the text. The CPMG decay is normalised to 74.6% at t = 0.

189

190

Figure 1 shows an example of data recorded for a sample of cement paste (w/c = 0.4; cured for 28 days). The top plot is the quadrature echo signal for a pulse gap τ = 12 μs together with a fit to a Gaussian echo centred on 2τ, representing the water used to create crystalline phases such as CH, and an exponential decay representing the mobile liquid. The central part of the figure shows the Gaussian amplitude back-extrapolated to $\tau = t_{\pi/2}$ [6] from which the combined and mobile water fractions are calculated. They are 25.4 ± 2.0% and 74.6 ± 2.0% respectively, in good agreement with previous results. The error is determined from repeat analyses across a range of samples. The lowest part of the figure shows the normalised CPMG decay and a four component, five free parameter constrained exponential fit as described in the previous section that decomposes the mobile water into components representing water in different pore types. The data is plotted in real (not magnitude) mode. Negative points of course do not plot on the log scale and the plateau beyond 10^4 μs is merely a reflection of the noise level. The amplitudes and relaxation times of the different components are presented in Table 1.

Assignment	Characteristic size (nm)	Amplitude (%)	T_2 relaxation time (μs)
Crystalline phases		25.4	10
Hydrate interlayers	1	22.9	185
Gel pores	3-5	49.1	555
Interhydrate pores	10-20	2.6	1665
Capillary pores	10^3	≈0.0	40000

Table 1. The assignment of water populations in "as-prepared" cement, with their characteristic pore sizes, NMR amplitudes and T_2 relaxation times.

[6] τ is measured pulse centre to pulse centre; so $t_{\pi/2}$ equates to zero gap between two pulses.

The negligible water fraction in capillary pores evidences, as has been observed before, the self-desiccation of samples of centimetre size during curing (*i.e*. pre-crushing in this work), notwithstanding that the samples are supposedly cured underwater [23].

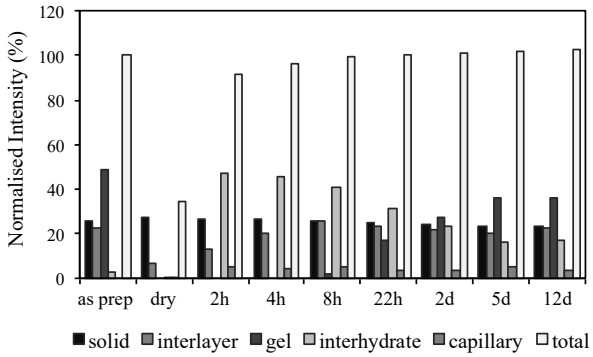

Figure 2. The evolution of water components of a sample: as prepared; after drying and then after 2, 4, and 8 hours and ≈1, 2, 5 and 12 days of rewetting expressed as a percentage of the NMR-total water in the "as-prepared" sample. The sample was oven dried at 60°C and 0.9 bar for 1 month.

Figure 2 shows the evolution of the different water fractions of a 28-day cured sample after drying and then periodically during the first two weeks of re-wetting. The sample is oven dried at 60°C for one month at 0.9 bar. It is evident that there is minimal mobile water remaining in the hydrate interlayer spaces and almost none in larger pores of the sample after drying compared to pre-drying. What follows concerns the subsequent rewetting. The discussion is further aided by inspection of Figure 3. This figure shows the combined water in the interlayer and gel pores and the combined water in interhydrate and capillary pores

as well as their sum, the total *mobile* water. We continue to use names already introduced to differentiate between pores of different size where the meaning is clear. However, since we will envisage that some gel pores collapse to a size comparable to the interlayer and so enlarge others gel pores to a size comparable to the interhydrate, we also introduce the terminology "finer porosity" to reflect pores less than about 10 nm and "coarser porosity" for pores greater than about 10 nm. Hence Figure 3 shows water in these two categories.

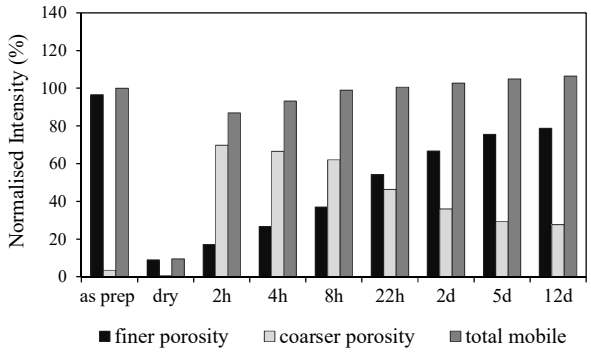

Figure 3. The evolution of mobile water in finer (<10 nm) and coarser (>10 nm) porosity for sample dried for 1 month at 60°C expressed as a percentage of the total mobile water.

The first observation is that the total filled porosity of the sample very quickly re-establishes itself to its pre-drying value, Figure 3. It gets to 87% in 2 hours and *exceeds* the pre-drying value after 1 day. This is reasonable because the crushed samples contain a significant number of capillary pores that are empty due to self-desiccation in the "as-prepared" material notwithstanding the so-called underwater curing. It is also possible that the largest

pores dried slightly during crushing. However, the former explanation is more likely since the increase is larger for a sealed-cured sample (data not shown here).

The second observation offers far greater insight. It is that the distribution of water between finer (<10 nm) and coarser (>10 nm) hydrate porosity changes dramatically during rewetting. It is seen most obviously in Figure 3. After 2 hours the amount of water in the finer porosity is approximately 17% the total pre-drying mobile water whereas the combined amount of water in coarser porosity is about 70% - about four times greater. This contrasts very strongly with pre-drying when the finer porosity was the dominant fraction, about 96%, while the coarser porosity was less than 4%, about 25 times smaller. However, by about 1 day, the volume of finer porosity water has increased dramatically while the coarser porosity water has decreased. The two fractions are approximately equal. At 12 days, the finer porosity water is approaching equilibrium, but has not regained the pre-drying volume, (80% compared to 96%). This indicates that only part of the refilling of the gel porosity is reversible on this timescale. The volume of coarser porosity water has continued to decrease correspondingly but remains much greater than pre-drying.

Figure 2 provides additional information. In the early stages of re-wetting, all the interlayer / gel pore water is seen as interlayer water. At 12 days, the amount of interlayer water is almost exactly equal to that pre-drying. The reduction in water in the finer porosity is associated almost entirely with the gel pores. For the coarser porosity, the increase in water in pores of interhydrate size (circa 20 nm) accounts almost exactly for the decrease in gel pore water. It is the capillary pores that account for the increase in the overall total of mobile water. This fact supports the idea that the total increase results from a filling of

257 previously unfilled capillary porosity. If the data had sufficient signal to noise, a proper
258 inverse Laplace transform might reveal details more precisely.

259

260 **(b) Severity of drying and C-S-H reswelling**

261 The same story does not carry over to a sample oven dried at 40°C and 0.9 bar for a short
262 period of just 2 days, Figure 4(d). Although, as before, the sample re-wets quickly, getting
263 near the pre-drying level within 2 hours, the distribution of water between the finer
264 porosity and coarser porosity remains essentially unchanged throughout the rewetting
265 period. There is no subsequent evolution of the amount of water in different pore types.

266 Potentially, two factors are at play in these phenomena: the severity of drying and the
267 duration of drying / storage. Table 2 seeks to separate the factors. It provides an indicator of
268 the drying severity, measured as the fraction of the interlayer and gel pore water removed
269 by drying. It is seen that oven drying for one month at 60°C is most severe. Drying at 40°C
270 for 2 days is least severe by this measure.

271

Drying	Duration of drying	Gel pore and interlayer water removed (%).
60°C oven at 0.9 bar	1 month	91
60°C oven at 0.9 bar	3 days	81
Progressively down to 15% RH at 20°C	1 month	64

Direct to 23% RH at 20°C	3 days	54
40°C oven at 0.9 bar	2 days	44

Table 2: The duration and severity of the different drying regimes, the latter measured by NMR as the fraction of finer porosity water removed from the cement paste.

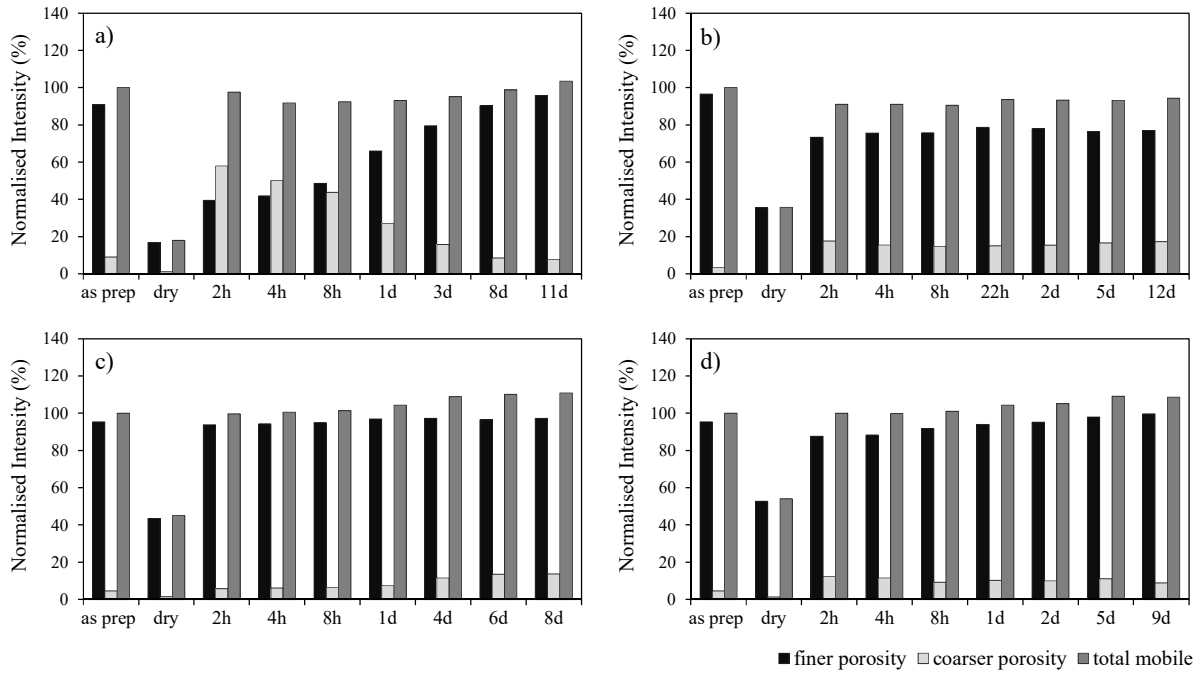

Figure 4: The combined finer and coarser pore water for samples dried: (a) at 60°C for 3 days; (b) slowly down to 15% RH; (c) directly to 23% RH; and (d) at 40°C for 2 days.

The data in other parts of Figure 4 allow us to explore the severity of drying more closely. Figure 4a is for a sample dried at 60°C for 3 days. The shorter drying period at the same temperature compared to the sample discussed in the previous section, is about 10% less severe (Table 2). Presumably in consequence, the sample dried for 3 days shows a C-S-H re-

organisation effect upon rewetting less strong than that for the sample dried for a month, Figure 3. Additionally, the amount of coarse porosity seen after 11 days rewetting is reduced while the amount of finer porosity is increased. Notwithstanding, these differences are much less than those discussed in the following paragraphs for samples dried in other ways. Hence, the result suggests that on the timescale of 3 days to one month, ~~timelapse during drying~~ the drying time is not an overly critical factor in driving initial changes.

The data shown in Figures 4b and c were obtained from samples that were dried progressively down to 15% at room temperature for 1 month and directly to 23% RH at room temperature for 3 days. Both drying regimes are less severe than the 60°C drying. Over half of the finer porosity water is removed. In both cases, the samples re-adsorb water to the overall pre drying level within the first two hours and do not show any subsequent redistribution. This is akin to the sample least severely dried at 40°C. However the *distribution* of water between finer and coarser porosity in the sample taken down to 15% RH is slightly different post-drying compared to pre-drying, whereas it is more-or-less the same in the taken to 23% RH. In the 15% RH sample, there is a little more water in coarser porosity, less in finer porosity post drying. Again we conclude that, at least for these drying conditions, the period of drying is not significant. However, what clearly differentiates between samples behaving as in Figure 3 from those in Figure 4d is whether or not the drying has significantly impacted the water content in the interlayer spaces. Drying at 60°C removes a large fraction of interlayer water; drying at 40°C does not.

(c) The second drying cycle.

The fact that both reversible and irreversible changes are seen in the foregoing data prompts the question as to what happens after a second cycle of drying and rewetting.

304 Samples either oven dried at 60°C for one month or progressively dried over saturated salt
305 solutions to 15% RH during 1 month and then rewet were both dried for a second cycle
306 using different combinations of the same two drying methods, so: oven-oven; RH salts-
307 oven; oven-RH salts; and RH salts-RH salts. They were then rewet for a second time. Figure 5
308 shows the second cycle results. To aid comparison with the first cycle, the figure also
309 includes the water fractions in different pore sizes before (*i.e.* as prepared) and after the 1st
310 cycle as previously described.

311 In the case of sample dried twice in the oven, Figure 5a, there is a clear second round of
312 evolution of the volume of water in different pore types. The initial invasion occurs during
313 the first two hours and takes the total mobile water to a level almost identical to that after
314 12 days of rewetting during the first cycle; that is a little more than in the "as-prepared"
315 sample. Again however, initially there is a greater fraction of water in the coarser porosity
316 than in the finer porosity. Once more as well, while the total remains approximately
317 constant, this division reverts over the subsequent few days to one with the greater fraction
318 in the finer porosity. Indeed, the values after 5 days are very close to those at the end of the
319 first cycle. This suggests that the second cycle changes correspond exclusively to the
320 reversible parts of the changes in the first cycle.

321 In the case of the sample dried above salt solutions in the first cycle and in the oven during
322 the second, Figure 5b, a time dependence of rewetting that was not seen in the first cycle is
323 now seen. The final state reached is very similar to that at the end of the first cycle. The
324 implication again is that the second cycle changes are reversible, even though the first cycle
325 was very different. In the case of the sample oven dried first cycle and above salt solutions
326 in the second, Figure 5c, the rewetting is quick and, once achieved in two hours, there is

very little change in either the total water content or in the division of water between the different pore types. The second cycle is behaving very similarly to the salt solution dried sample in the first. Notwithstanding, there is a very small change in the division of water between the pores at the end of the first and second cycles. The finer porosity water fraction in the second cycle is a little lower than in the first; the coarser porosity fraction correspondingly more. However this difference is small and, overall, it seems that most, if not all, of the irreversible changes occurred in the first cycle. Given that drying above salt solutions produced no time varying organisation of the porosity in the first or second cycle when combined with oven drying in the other cycle, then it seems unlikely that it will create time dependence in a sample dried above salt solutions in both cycles. This is shown to be the case, Figure 5d.

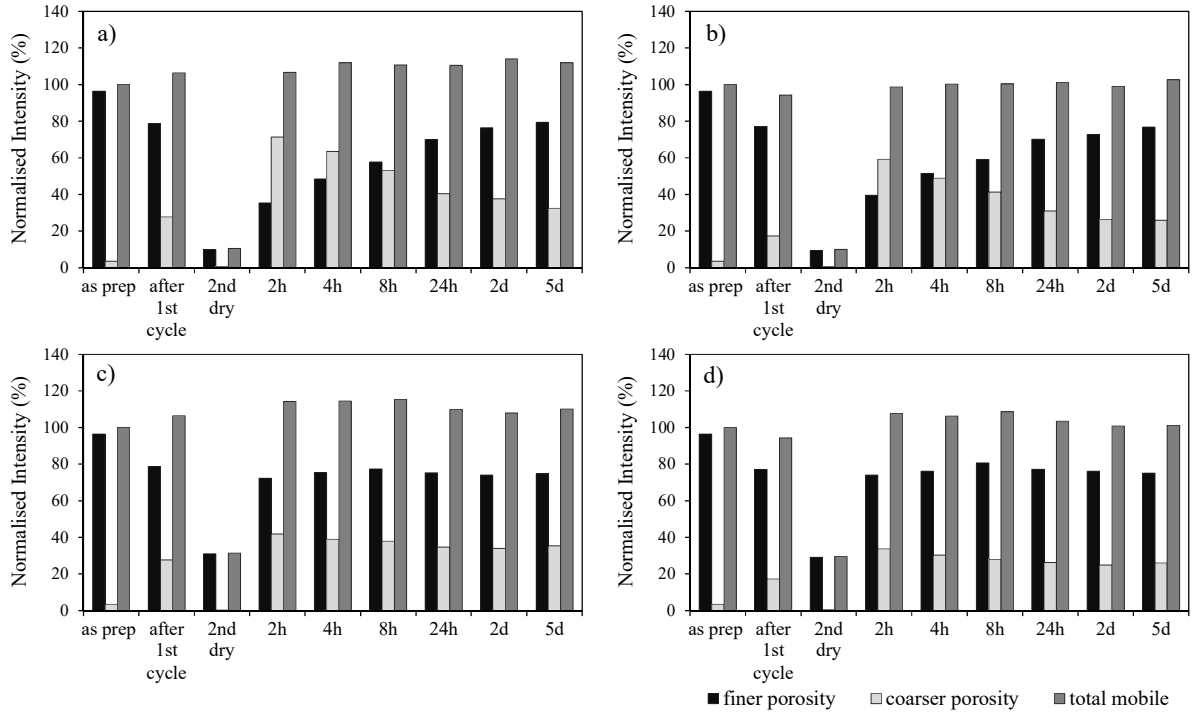

Figure 5. The evolution of the finer and coarser pore water during a second cycle of drying and rewetting: (a) oven dried 1st cycle – oven dried 2nd cycle; (b) dried

above salt solutions – oven dried; (c) oven – salts; and (d) salts – salts. To aid recognition of reversible and irreversible effects the first column is the "as prepared" sample and the second column the sample at the end of the first cycle.

338

339 **Discussion**

340 An explanation of our data is drawn schematically in Figure 6. The schematic is for a sample
341 in which the gel porosity is completely emptied of water and then refilled. Figure 6a shows
342 some C-S-H sheets separated by interlayer spaces. Gel pores are seen between regions of
343 locally aggregated sheets. The gel pores are filled with water, drawn as circles. The
344 interlayer spaces also contain water but this is not shown. The gel pores are a few (3-5)
345 nanometres in size. Interhydrate pores are slightly larger and are original-mix water filled
346 spaces between regions of C-S-H into which further C-S-H could possibly grow. However
347 these are not drawn. As water is removed from the system, Figure 6b, we imagine that
348 surface energy or disjoining pressure forces distort the local arrangement of the sheets so as
349 to "zip them up" into locally-thicker stacks. The surface forces overcome local bending
350 stresses in order to do this. The result is the average gel pore size increases although the
351 total volume does not, at least to a degree measurable by NMR. When water reinvades the
352 sample, it initially finds larger pores that are apparently more comparable to interhydrate
353 pores in size. With time, the "zipped" sheets "unzip". That is they relax in response to the
354 changed balance of surface forces and bending stresses. Something closer to the original
355 microstructure re-appears.

356 It is very noticeable that we see this result most prominently with the two most severe
357 drying methods: 2-3 days and 1 month at 60°C. We do not see it with the least severe
358 methods. A key difference is that the more severe drying removes a significant fraction
359 (over half) of the interlayer water. Perhaps with less severe drying, sufficient water is
360 retained in the smallest spaces to prevent large surface energy or disjoining pressure forces
361 from building up. Local "zipping" of sheets cannot occur. The vapour pressure of water is
362 about 3 times higher at 40°C than at 20°C, and 9 times higher at 60°C. So, if the laboratory
363 atmosphere is circa 60% RH at 20°C, then a sample in an unsealed oven at 60°C experiences
364 about 7% RH, quite sufficient to impact the interlayer in an equilibrated sample. However,
365 40°C leads to 20% RH and is much less impactful. It is striking that our results show the
366 greatest effects for the most severely dried samples but that the drying rate does not seem
367 to be a primary indicator of change. This contrasts with the work of Maruyama *et al*. [15]
368 who emphasise the importance of drying rate on the shrinkage strain of hardened cement
369 paste during the first desorption process although the timescales in this work do not extend
370 as far as those explored by Maruyama *et al*.

371 One surprise in our data is that we do not see more interlayer water in samples that show
372 the evolving porosity at the end of the rewetting period compared to pre-drying. Figure 6
373 makes clear that if the average gel pore size at the end is increased, then this increase is
374 accompanied by locally thicker stacks of layers. The number of interlayers is increased. One
375 explanation is simply that we are unable to resolve differences of this magnitude. However,
376 we think this is unlikely. Another explanation is that some of the original water that is
377 removed from interlayer spaces is not replaced. This decrease in water per interlayer
378 compensates for the increase in the number of interlayers.

379 It is well known that the first drying cycle of cement paste yields a mixture of reversible and
380 irreversible changes in sorption isotherms and shrinkage. However, these differences tend
381 to be associated with the high RH end of the drying spectrum [4,15,16]. To first order, only
382 reversible changes are seen after the first cycle. We note that in this work, the changes are
383 associated with the most severe drying, that is the low RH end of the spectrum. However,
384 there are reversible and irreversible changes. Close comparison of the data in Figures 3 and
385 5 suggests that irreversibility continues to be associated with the first cycle only.

386 Maruyama *et al.* discuss the shrinkage mechanism in terms of Jennings' colloidal model of
387 cement microstructure [4]. They conclude that the increase in porosity due to larger pores
388 occurs by the flocculation of C-S-H globules whereas the decrease in porosity due to smaller
389 pores arises from densification of the C-S-H through the loss of interlayer water. Thus they
390 are seen as different processes. Moreover they are believed to occur in different ranges of
391 RH. This is because the Kelvin Laplace equation links RH to the size of emptying pores. If the
392 increase in apparent proper (micron) capillary porosity that we see through the filling of
393 previously empty pores (Figure 2) is removed from the equation, then the growth in coarser
394 porosity is almost exactly matched by the loss of finer porosity. Given that Maruyama *et al.*
395 describe different processes associated with different parts of the microstructure and
396 different RH ranges, it is therefore surprising that the growth in finer porosity that we see in
397 re-wetting is so closely mirrored by the decline in coarser porosity. It seems much more
398 likely to us that they are opposite sides of a single process. Such a single process can be built
399 on rearrangements of C-S-H sheets at the gel pore scale based on a Feldman and Sereda
400 type micro-structural model [17] as we have depicted in Figure 6. However, our explanation
401 is unable to explain the conclusion of Maruyama *et al.*: that the two processes come about

402 at different ranges of RH. Macroscopic drying shrinkage, to which NMR is not sensitive, may
403 provide part of the answer.

404

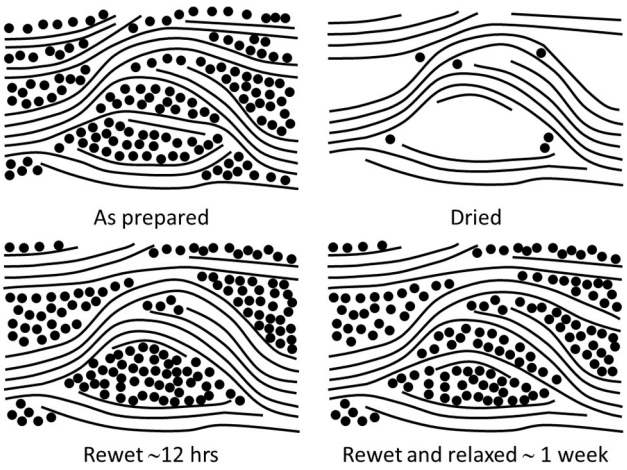

Figure 6. Top left: A schematic of the water in the gel pores of an "as-prepared" paste. The solid lines are the hydrate backbone sheets of the C-S-H gel. The circles are water molecules. The interlayer water between the sheets is not shown. As a guide to scale, the layer spacing is about 1.5 nm. Top right: The hydrate after sufficient drying to remove almost all the water from the gel pores. Surface forces cause some sheets to distort and "zip-up". Bottom left: the same structure shortly after rewetting. The exact same amount of water as top left is shown, but it is now in fewer, and, on average, slightly larger pores. Bottom right: after a few days the hydrate partially relaxes closer to the original microstructure. Again, the same amount of water is shown. The pores are smaller.

405

406

Notwithstanding the comments immediately above, there is ongoing controversy as to whether or not C-S-H is a quasi continuous [17] or colloidal particle like layered structure [4]. While the data in this work has been interpreted in terms of the quasi continuous model, it would be possible to rework the discussion in terms of the colloidal model. Nothing in the new data is incompatible with either.

Conclusion

We have provided compelling NMR evidence for the redistribution of porosity between fine (<10 nm) and coarser (>10 nm) spaces in cement gel occasioned by cycles of drying and rewetting. In “well” dried material, coarse (20 nm) pores are created at the expense of collapsing gel pores. When the sample is rewet, these effects are reversed over a period of days. The degree of the change is linked to the severity of the drying. In a first sorption cycle, part of the redistribution is reversible, part is not. In a second cycle the changes appear to be entirely reversible. Aspects of the results mirror observations of macroscopic length changes made by Maruyama *et al*. However, we suggest that a completely self-consistent picture of all the published data, by us and by others, has not yet emerged. Future experiments with much finer control of the drying rate and drying severity as well as measurements targeted on the very first minutes of rewetting might further elucidate the matter.

Acknowledgements

The research leading to these results is partly funded from the European Union Seventh Framework Programme (FP7 / 2007-2013) under grant agreement 264448.

References

[1] Z.P. Bažánt, W.J. Raftshol, Effect of cracking in drying and shrinkage specimens, Cem. Conc. Res. 12 (1982) 209–226.

[2] W. Hansen, Drying Shrinkage Mechanisms in Portland Cement Paste, J. Am. Ceram. Soc. 70 (1987) 323–328. doi:10.1111/j.1151-2916.1987.tb05002.x.

[3] F.H. Wittmann, Heresies on shrinkage and creep mechanisms, in: T. Tanabe, K. Sakata, H. Mihashi, R. Sato, K. Maekawa, H. Nakamura (Eds.), Proceedings of the 8th International Conference on Creep, Shrinkage and Durability Mechanics of Concrete and Concrete Structures, 2008: pp. 3–9.

[4] H.M. Jennings, Refinements to colloid model of C-S-H in cement: CM-II, Cem. Conc. Res. 38 (2008) 275–289. doi:10.1016/j.cemconres.2007.10.006.

[5] R.A. Helmuth, D.H. Turk, Reversible and Irreversible Drying Shrinkage of Hardened Portland Cement and Tricalcium Silicate Pastes, J. PCA Res. Dev. Lab. 9 (1967) 8–21.

[6] A.C.A. Muller, K.L. Scrivener, A.M. Gajewicz, P.J. McDonald, Densification of C–S–H Measured by 1H NMR Relaxometry, J. Phys. Chem. C. 117 (2013) 403–412. doi:10.1021/jp3102964.

[7] J.R. Zimmerman, W.E. Brittin, Nuclear Magnetic Resonance Studies in Multiple Phase Systems: Lifetime of a Water Molecule in an Adsorbing Phase on Silica Gel, J. Phys. Chem. 61 (1957) 1328–1333. doi:10.1021/j150556a015.

[8] K.R. Brownstein, C.E. Tarr, Spin-lattice relaxation in a system governed by diffusion, J. Magn. Reson. 26 (1977) 17–24. doi:10.1016/0022-2364(77)90230-X.

[9] F. D'Orazio, J.C. Tarczon, W.P. Halperin, K. Eguchi, T. Mizusaki, Application of nuclear magnetic resonance pore structure analysis to porous silica glass, J. Appl. Phys. 65

(1989) 742. doi:10.1063/1.343088.

[10] A. Muller, K.L. Scrivener, A.M. Gajewicz, P.J. McDonald, Use of bench-top NMR to measure the density, composition and desorption isotherm of CSH in cement paste, Microporous and Mesoporous Materials. 178 (2013) 99–103. doi:10.1016/j.micromeso.2013.01.032.

[11] A.M. Gajewicz, Characterisation of cement microstructure and pore-water interaction by ^{1}H nuclear magnetic resonance relaxometry, PhD thesis, University of Surrey, 2014.

[12] A. Valori, P.J. McDonald, K.L. Scrivener, The morphology of C–S–H: Lessons from 1H nuclear magnetic resonance relaxometry, Cem. Conc. Res. 49 (2013) 1–17. doi:10.1016/j.cemconres.2013.03.011.

[13] A.C.A. Muller, J. Mitchell, P.J. McDonald, Proton NMR Relaxometry, in: K.L. Scrivener, R. Snellings, B. Lothenbach (Eds.), A Practical Guide to Microstructural Analysis of Cementitious Materials, 1st ed., CRC Press, 2016: pp. 287–349.

[14] N. Fischer, R. Haerdtl, P.J. McDonald, Observation of the redistribution of nanoscale water filled porosity in cement based materials during wetting, Cem. Conc. Res. 68 (2015) 148–155. doi:10.1016/j.cemconres.2014.10.013.

[15] I. Maruyama, Y. Nishioka, G. Igarashi, K. Matsui, Microstructural and bulk property changes in hardened cement paste during the first drying process, Cem. Conc. Res. 58 (2014) 20–34. doi:10.1016/j.cemconres.2014.01.007.

[16] H.M. Jennings, A. Kumar, G. Sant, Quantitative discrimination of the nano-pore-structure of cement paste during drying: New insights from water sorption isotherms, Cem. Conc. Res. 76 (2015) 26–36. doi:10.1016/j.cemconres.2015.05.006.

[17] R.F. Feldman, P.J. Sereda, A new model for hydrated Portland cement and its

practical implications, Engineering Journal. 53 (1970) 53–59.

[18] A. Carotenuto, M. Dell'Isola, An experimental verification of saturated salt solution-based humidity fixed points, Int J Thermophys. 17 (1996) 1423–1439. doi:10.1007/BF01438677.

[19] P.W. Winston, D.H. Bates, Saturated Solutions For the Control of Humidity in Biological Research, Ecology. 41 (1960) 232. doi:10.2307/1931961.

[20] P.J. McDonald, V. Rodin, A. Valori, Characterisation of intra- and inter-C–S–H gel pore water in white cement based on an analysis of NMR signal amplitudes as a function of water content, Cem. Conc. Res. 40 (2010) 1656–1663. doi:10.1016/j.cemconres.2010.08.003.

[21] A.C.A. Muller, K.L. Scrivener, J. Skibsted, A.M. Gajewicz, P.J. McDonald, Influence of silica fume on the microstructure of cement pastes: New insights from 1H NMR relaxometry, Cem. Conc. Res. 74 (2015) 116–125. doi:10.1016/j.cemconres.2015.04.005.

[22] L. Monteilhet, J.P. Korb, J. Mitchell, P.J. McDonald, Observation of exchange of micropore water in cement pastes by two-dimensional T_2-T_2 nuclear magnetic resonance relaxometry, Phys. Rev. E. 74 (2006) 061404. doi:10.1103/PhysRevE.74.061404.

[23] H. Chen, M. Wyrzykowski, K. Scrivener, L. Pietro, Modeling of internal relative humidity evolution in cement pastes at early age, in: K.V. Breugel, W. Sun, C. Miao (Eds.), Second International Conference on Microstructural-related Durability of Cementitious Composites, RILEM Publlcations, Amsterdam, 2012: pp. 342–349.